CHINESE OPTICS LETTERS

Vol. 19, No. 11 | November 2021

Gain and laser performance of heavily Er-doped silica fiber fabricated by MCVD combined with the sol-gel method

Qiubai Yang (阳求柏)[1,2,†], Yan Jiao (焦 艳)[2,†], Chunlei Yu (于春雷)[2,3*], Chongyun Shao (邵冲云)[2], Fengguang Lou (楼风光)[2], Shikai Wang (王世凯)[2], Lei Zhang (张 磊)[2], Qiuhong Yang (杨秋红)[1], and Lili Hu (胡丽丽)[2,3**]

[1] School of Materials Science and Engineering, Shanghai University, Shanghai 200444, China

[2] Key Laboratory of High Power Laser Materials, Shanghai Institute of Optics and Fine Mechanics, Chinese Academy of Sciences, Shanghai 201800, China

[3] Hangzhou Institute for Advanced Study, University of Chinese Academy of Sciences, Hangzhou 310024, China

*Corresponding author: sdycllcy@163.com

**Corresponding author: hulili@siom.ac.cn

Received February 7, 2021 | Accepted April 27, 2021 | Posted Online August 18, 2021

In this work, a heavily Er-doped fiber with an 8 μm core diameter and a numerical aperture of 0.13 was prepared by the modified chemical vapor deposition (MCVD) technique combined with the sol-gel method. The background loss and absorption coefficient at 1530 nm were measured to be 20 dB/km and 128 dB/m, respectively. Thanks to the sol-gel method, the fiber showed a good doping homogeneity, which was confirmed through unsaturable absorption measurement. The net gains of three 25, 45, and 75-cm-long fibers were measured in the range of 1520 to 1600 nm, and the highest gain reached above 23 dB at both 1530 and 1560 nm in 25 and 75-cm-long fibers, respectively. The short-cavity laser performance was measured using centimeter-scale fibers. The maximum output power of 12 mW was demonstrated in a 6.5-cm-long active fiber with a slope efficiency of 20.4%. Overall, the prepared heavily Er-doped silica fiber is a promising item to be applied in a high-repetition-rate or single-frequency fiber laser.

Keywords: erbium-doped fiber; short-cavity fiber laser; sol-gel method.

DOI: 10.3788/COL202119.110603

1. Introduction

Since the 90s, Er-doped fiber amplifiers (EDFAs) play an important role in modern optical telecommunications. Besides this, in recent years, high-repetition-rate (HRR) or single-frequency (SF) Er-doped fiber lasers (EDFLs) are widely applied in some specific fields, owing to their eye safety and high atmospheric transmission, such as remote sensing, LIDAR, and gravitational wave detection[1–11]. A short-length laser cavity can not only suppress nonlinear effect, but also increase the repetition rate and longitudinal mode spacing[12–16]. Therefore, enhancing Er^{3+} ions doping concentration in Er-doped fibers (EDFs) to shorten the active fiber length is demanded for HRR and SF fiber lasers.

However, for silica-based EDFs manufactured by modified chemical vapor deposition (MCVD), the doping concentration is limited by Er^{3+} ion clusters induced quenching (CIQ), which is detrimental to emission properties[17–20]. Codoping with the "network modifiers" (such as Al^{3+} or P^{5+}) was demonstrated to be an efficient and feasible approach to adapt the rigid network in silica and enhance the solubility of Er ions[17,21,22]. However, the very high Al content is unfavorable to the single-mode operation and is also difficult to be obtained in an MCVD prepared fiber. Thus, the concentration of Er ions in silica fiber performed by MCVD is still typically lower than ~0.5% (mass fraction).

Several researchers focus on non-silica fibers[14,15,23–25]. Although the high background loss might be ignored in a short-cavity laser regime, the environmental stability and the difficulty of splicing limit their application in all-fiber laser and amplifier schemes. For solving these problems, researchers combined an Er-doped phosphate core and silica cladding together[26,27]. The silica cladding can be spliced easily with other commercial silica fibers and guarantees the mechanical strength. However, owing to the large differences between core and cladding glass in transition temperature and thermal expansion coefficient, mutual diffusion between core and cladding is inevitable. The diffusion of glass leads to not only transversal but also longitudinal inhomogeneities in the refractive index and rare earth concentration, which might deteriorate beam quality and gain performance.

Several fiber manufacturing processes based on the CVD process have been developed to ensure uniform dispersion of Er ions, such as surface plasma chemical vapor deposition

(SPCVD)[13,28], direct nanoparticle deposition (DND)[29], nanoparticle doping (ND)[19], and *in-situ* nano solution doping[30]. In recent years, our group fabricated a heavily Er-doped silica fiber without quenching effects using the sol-gel method combined with high-temperature sintering (sol-gel EDF, SG-EDF)[31]. The merit of the sol-gel method is that it can disperse Er ions effectively to achieve molecular level doping homogeneity and thus decrease the severe performance degradation due to CIQ. However, high background loss is easily caused by contamination during the high-temperature sintering process.

In this Letter, we introduced an MCVD combined with sol doping technology to fabricate heavily doping silica fiber. This fiber fabrication method combines the advantage of low-loss preparation of MCVD and the sol-gel merit of high doping homogeneity. Based on this technique, we prepared a heavily Er-doped silica fiber (MCVD and SG-EDF, MS-EDF). The core absorption and background loss were measured using the cut-back method. The unsaturable absorptions of the MS-EDF and the SG-EDF were measured to estimate the CIQ effect. Also, gain and short-cavity lasing properties of the MS-EDF were invested and discussed in all-fiber schemes.

2. Fiber Fabrication

The method of preparing the Er^{3+}-doped silica preform is shown in Fig. 1. Firstly, a porous silica layer was deposited in a chemically polished silica tube (F300, Heraeus) with $SiCl_4$ flow of 200 mL/min. The temperature of oxy-hydrogen burner is set to 1500°C to ensure uniform porosity. After pure silica soot deposition, we immersed it in the Er/Al co-doped transparent sol for 1 h of soaking. The sol composition is $0.3Er_2O_3 \cdot 3Al_2O_3 \cdot 96.7SiO_2$ in molar ratio, and the preparation of rare-earth-doped transparent sol was already described in detail in our previous works[32]. Subsequently, the soot is dried in a flow of Cl_2–O_2 gas mixture at the temperature of 1000°C to reduce the OH content of core glass. For the sol doping method, the carbon removal process is necessary. Therefore, after the sol is drained, the soot tube continued to be heated to 1200°C in the presence of the He–O_2 gas mixture to remove residual carbon. After that, the porous soot tube was consolidated and collapsed into a transparent solid fiber preform by heating it to a temperature of 2200°C with a moving burner. Finally, the preform was drawn into fiber at the optimized conditions to guarantee high mechanical strength.

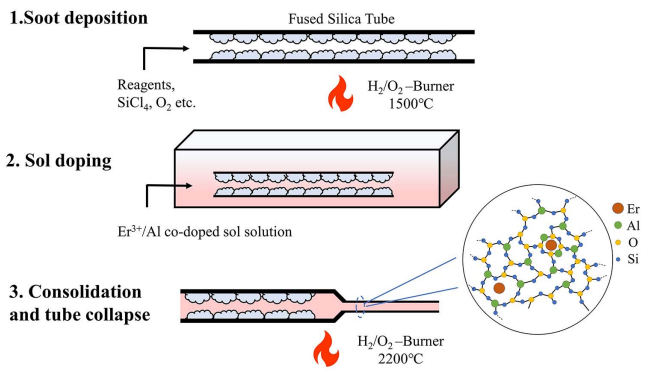

Fig. 1. Schematic diagram of fiber preform fabrication.

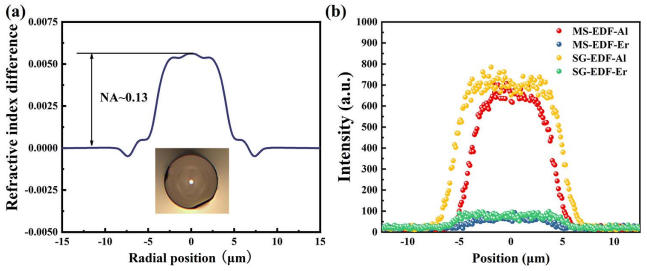

Fig. 2. (a) Radial refractive index profile. Inset: micrograph of MS-EDF cross section. (b) Concentrations of Al^{3+} and Er^{3+} in the MS-EDF and SG-EDF from EPMA measurement.

Figure 2(a) shows the radial refractive index profile (RIP) measured by an optical fiber analyzer (IFA-100). It is shown that there is no central dip in the RIP, and the refractive index fluctuation is lower than 3×10^{-4}. The refractive index difference with respect to the pure silica glass is about 5.5×10^{-3} thanks to the sol-gel method decreasing the Al content. The corresponding numerical aperture (NA) is 0.13, which can achieve single-mode operation with an ~8 μm core diameter for application at 1.5 μm. The concentration distribution of Al^{3+} and Er^{3+} in both MS-EDF and SG-EDF measured by an electron probe micro analyzer (EPMA, JEOL, JXA-8230) is shown in Fig. 2(b). For the SG-EDF, the concentrations of Er^{3+} and Al^{3+} in the core glass rod were measured to be 16,200 ppm (parts per million) and 25,200 ppm through inductively coupled plasma optical emission spectrometry (ICP-OES, radial-view Thermo iCAP 6300), respectively. The concentrations of Er^{3+} and Al^{3+} in the MS-EDF core are a little bit lower than that in the SG-EDF and thus are estimated to be 15,000 ppm (by weight) and 24,000 ppm (by weight), respectively. The dilution effect of doping into silica soot may be responsible for the relatively low concentration.

The core background loss and absorption spectra were measured with a white light source and an optical spectrum analyzer (OSA) by the cut-back method. In Fig. 3(a), we plotted the background loss spectra of the heavily EDF. The background loss is about 20 dB/km at 1100 nm, which is much lower than the

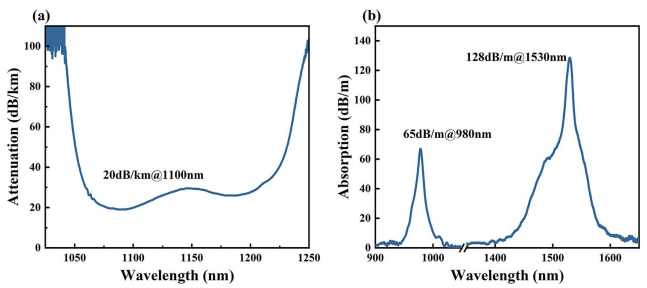

Fig. 3. (a) Background loss and (b) absorption of the MS-EDF.

200 dB/km of the SG-EDF reported in Ref. [21], owing to the low-loss MCVD fabrication process. The core absorption spectrum was measured using a short fiber, and the result was plotted in Fig. 3(b). The core absorption coefficients of the MS-EDF at 980 nm and 1530 nm were about 65 dB/m and 128 dB/m, respectively.

3. Experiments and Results

The lifetime of the metastable level in the clustered Er^{3+} ions is several orders of magnitude shorter (50 ns–10 μs) than that in isolated Er^{3+} ions, which is due to so-called CIQ[20,33]. The simplified energy levels of the isolated Er^{3+} ions and the clustered Er^{3+} ions are shown in Fig. 4(a). After absorbing pump power, Er^{3+} ions are activated into the upper level $^4I_{11/2}$ and transmitted to the sublevel $^4I_{13/2}$ rapidly. For isolated Er^{3+} ions, because it takes time to relax back to the ground state, the number of ions in the ground state could not be replenished in time, and then the absorption is saturated. But, for the clustered ions, the quenching effect leads to the relaxation of the excited clusters being so fast that they are difficult to be excited, and most of them remain in the ground state absorbing pump power[20]. Thus, the absorption of the clustered Er^{3+} ions is unsaturable, even if the pump power is very large. Therefore, in many papers, the proportion of the clustered ions in EDFs was estimated through unsaturable absorption measurement[18,20,29].

The unsaturable absorptions of the MS-EDF and the SG-EDF at 976 nm are shown in Fig. 4(b). The lengths of two fibers were chosen for providing the same absorption of pump power at 976 nm, and it can be seen in Fig. 4(b) that the maximum small-signal absorptions of two fibers are both about 22 dB. With the input laser power increasing, the absorption was decreased rapidly and became stable gradually. The stable value is called unsaturable absorption, and the unsaturable absorption fraction is the ratio of unsaturable absorption to the maximum absorption. This part of absorbed pump power cannot transfer to laser power, and thus it can be considered as "excess background loss" to a certain extent. When the injected pump power is 199 mW, the absorption of the MS-EDF is 9.3 dB, thus the unsaturable absorption fraction is ~43.2%. However, for the SG-EDF, the unsaturable absorption fraction is 54.9%. The reason why the unsaturable absorption fraction of the MS-EDF is smaller than that of the SG-EDF can be attributed to the doping concentration difference, which can also be found from the EPMA results and absorption coefficient.

We also measured the fluorescence decay of the $^4I_{13/2}$ energy level in the MS-EDF and the SG-EDF, which was core pumped using a pulsed 980 nm laser. The decay curve was recorded using an InGaAs photon detector (DET20C2, Thorlabs) and an oscilloscope (DSOX6002A, Keysight). It is seen from Fig. 4(c) that the lifetime of the two fibers is around 10 ms, showing no obvious lifetime shortening. Therefore, from the results of unsaturable absorptions and fluorescence decay measurements, the MS-EDF has a high doping homogeneity without concentration quenching.

As is shown in Fig. 5(a), the gain properties of the MS-EDF were evaluated with an all-fiber EDFA setup. The EDFA was seeded by a tunable light source (TSL) operated in the C + L band. An optical isolator (ISO) was placed after the seed source to protect the TSL from backward propagating light. The signal optical power injected into the EDFA was fixed to be −30 dBm through adjusting the seed power. The EDF was core pumped by a single-mode 976 nm laser diode (LD) in a forward pumping configuration via a 980/1550 nm wavelength division

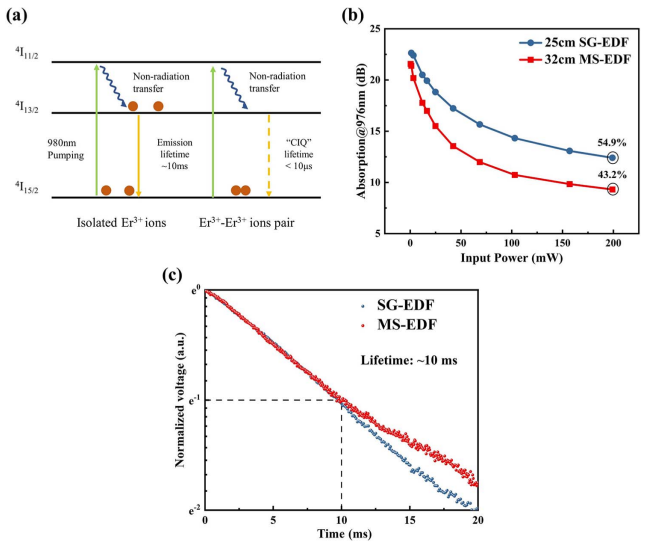

Fig. 4. (a) Simplified energy level diagram of isolated Er^{3+} ions and Er^{3+}-Er^{3+} pairs with an excitation at 980 nm. (b) Unsaturable absorptions at 976 nm of a 25 cm SG-EDF (blue) and a 32 cm MS-EDF (red). (c) Fluorescence decay curves obtained from the two fibers.

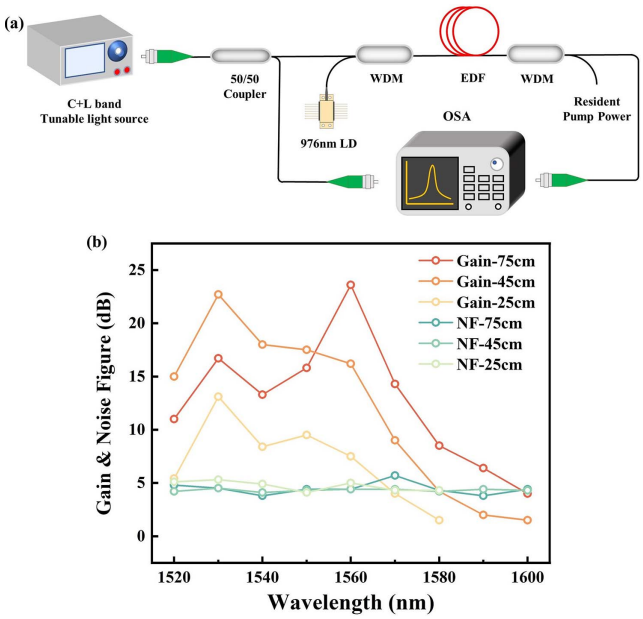

Fig. 5. (a) Schematic of EDFA experiment. (b) Dependence of the gain and NF of the MS-EDF on the wavelength with different fiber lengths.

multiplexer (WDM). After the active fiber, another WDM was used to split the amplified signal and residual pump light. The spectra of the input signal and the amplified signal were measured with an OSA to calculate the gain and the noise figure (NF). In the measurement, the insert loss and propagation loss of the whole device have been taken into account.

Figure 5(b) shows the signal gain and NF from 1520 to 1600 nm under 500 mW launched pump power and −30 dBm input signal power for three different fiber lengths of 75, 45, and 25 cm. The step size of the wavelength was 10 nm. The NF of the MS-EDF at all measured wavelengths is less than 6 dB, showing an excellent noise performance. It can be seen that the gain peak wavelength of the shorter fiber is located at 1530 nm, and the maximum gain red shifted to 1560 nm with longer fiber. The small-signal gain at 1530 nm was ∼0.5 dB/cm obtained in both 25 and 45-cm-long MS-EDFs. The maximum gain up to 23.6 dB with an NF of 4.4 dB was obtained by the 75-cm-long MS-EDF at 1560 nm.

The short-cavity laser performance was investigated, employing a short linear cavity scheme as in Fig. 6(a). A laser cavity was formed by a pair of fiber Bragg gratings (FBGs) fabricated in a standard 1.5 μm single-mode fiber (SMF-28e, Corning). The reflectivity of the low-reflectivity (LR) FBG is ∼50%, which is centered at 1533.66 nm with a 3 dB bandwidth of 0.15 nm. The high-reflectivity (HR) FBG is centered at 1533.65 nm with a 3 dB bandwidth of 0.45 nm, and its reflectivity is above 99%. A backward pumping configuration was applied this time to easily split the laser power and residual pump power via a WDM. An ISO was spliced to the 1550 nm end of the WDM to block the backward propagating light. The laser power and residual pump power were recorded by two optical power meters, respectively, and the laser spectrum was measured using an OSA.

The dependence of laser output power on absorbed pump power for five different fiber lengths (3.7, 5.0, 5.7, 6.5, and 8.0 cm) is illustrated in Fig. 6(b). With the increased fiber length, the slope efficiency initially increases from 13.6% to 20.4%, then decreases from 20.4% to 13.6%. The highest slope efficiency of 20.4% and output power of 11.9 mW were obtained in a 6.5-cm-long MS-EDF under 81 mW absorbed pump power. The slope efficiency of 20.4% is higher than the value reported for SG-EDF (12%, in Ref. [31]), and it can be attributed to lower background loss.

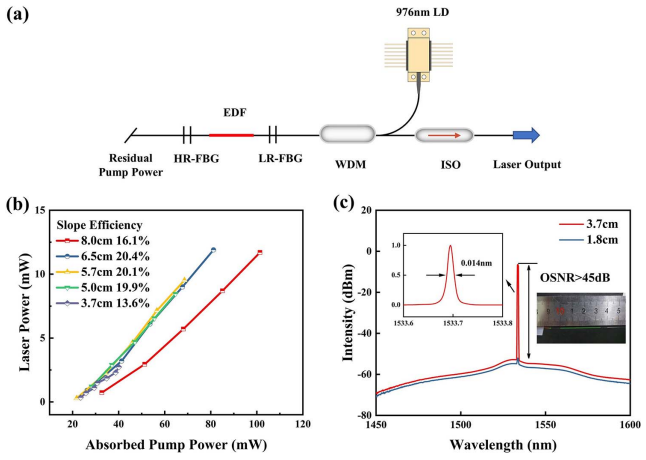

Fig. 6. (a) Schematic of short-cavity laser experiment. (b) Dependence of laser output power on absorption pump power for different fiber length. (c) Laser spectra of 3.7 and 1.8-cm-long fibers. Inset: the enlarged and normalized spectrum (left) and the picture of the laser cavity (right) using the 3.7-cm-long MS-EDF.

For a longer fiber, the signal power was reabsorbed by an extra active fiber, which results in lower laser efficiency. For a shorter length fiber, it is very difficult to absorb enough pump power and provide enough gain, resulting a larger threshold and lower slope efficiency. The output spectra of a 3.7 cm and a 1.8 cm MS-EDF are shown in Fig. 6(c), and the left inset is the enlarged and normalized laser spectrum, which was measured at a resolution of 0.02 nm. The laser spectrum of the 3.7 cm MS-EDF was centered at 1533.7 nm with a 0.014 nm spectrum linewidth full width at half-maximum (FWHM), and it shows great optical signal-to-noise ratio (OSNR) performance. Meanwhile, it can be noted that the 1.8-cm-long MS-EDF could not achieve effective lasing due to insufficient gain, although we maximized the pump power.

4. Conclusion

In this Letter, we proposed a technique to fabricate heavily EDFs combining commercial MCVD with the sol-gel method. The proposed technique can achieve a uniform dispersion of Er ions in a silica matrix, and the clustered Er^{3+} ion fraction was estimated by unsaturable absorption measurement. The peak absorption coefficient is ∼128 dB/m at 1530 nm. The background loss of the MS-EDF is measured to be ∼20 dB/km at 1100 nm and compatible to commercial EDFs. The net gain coefficient of the MS-EDF can reach 23 dB at both 1530 and 1560 nm through adjusting the fiber length. Thanks to the low background loss and unsaturable absorption, our MS-EDF shows great laser performance. The maximum average power of 12 mW and slope efficiency of 20.4% were successfully obtained in a 6.5-cm-long MS-EDF. At a fiber length of 3.7 cm, an effective lasing was obtained with an OSNR up to 45 dB and an FWHM of 0.014 nm. We believe our MS-EDF can be a promising candidate for HRR and SF fiber lasers. At the same time, the new fiber fabrication technique can also be applied to other rare-earth fibers, such as ytterbium and thulium.

Acknowledgement

This work was supported by the National Key R&D Program of China (No. 2020YFB1805900), National Natural Science Foundation of China (NSFC) (No. 62005297), Shanghai Sailing Program (No. 20YF1455300), and Shanghai Science International Cooperation Project (No. 18590712900).

†These authors contributed equally to this work.

References

1. C. C. V. Philippov, Y. Jeong, C. Alegria, J. K. Sahu, and J. Nilsson, "High-energy in-fiber pulse amplification for coherent lidar applications," Opt. Lett. **29**, 2590 (2004).
2. W. Lee, J. Geng, S. Jiang, and A. W. Yu, "1.8 mJ, 3.5 kW single-frequency optical pulses at 1572 nm generated from an all-fiber MOPA system," Opt. Lett. **43**, 2264 (2018).
3. C. Lei, H. Feng, Y. Messaddeq, and S. LaRochelle, "Investigation of C-band pumping for extended L-band EDFAs," J. Opt. Soc. Am. B **37**, 2345 (2020).
4. J. L. Y. Liu and W. Chen, "Eye-safe, single-frequency pulsed all-fiber laser for Doppler wind lidar," Chin. Opt. Lett. **9**, 090604 (2011).
5. S. Han, H. Jang, S. Kim, Y.-J. Kim, and S.-W. Kim, "MW peak power Er/Yb-doped fiber femtosecond laser amplifier at 1.5 μm center wavelength," Laser Phys. Lett. **14**, 080002 (2017).
6. V. Kuhn, D. Kracht, J. Neumann, and P. Weßels, "Er-doped single-frequency photonic crystal fiber amplifier with 70 W of output power for gravitational wave detection," Proc. SPIE **8237**, 82371G (2012).
7. O. Varona, M. Steinke, J. Neumann, and D. Kracht, "All-fiber, single-frequency, and single-mode Er^{3+}:Yb^{3+} fiber amplifier at 1556 nm core-pumped at 1018 nm," Opt. Lett. **43**, 2632 (2018).
8. M. M. Khudyakov, D. S. Lipatov, A. N. Gur'yanov, M. M. Bubnov, and M. E. Likhachev, "Highly efficient 3.7 kW peak-power single-frequency combined Er/Er-Yb fiber amplifier," Opt. Lett. **45**, 1782 (2020).
9. Z. Guo, Q. Hao, J. Peng, and H. Zeng, "Environmentally stable Er-fiber mode-locked pulse generation and amplification by spectrally filtered and phase-biased nonlinear amplifying long-loop mirror," High Power Laser Sci. Eng. **7**, e47 (2019).
10. J. Bogusławski, G. Soboń, R. Zybała, and J. Sotor, "Towards an optimum saturable absorber for the multi-gigahertz harmonic mode locking of fiber lasers," Photon. Res. **7**, 1094 (2019).
11. X. Chen, Y. Gao, J. Jiang, M. Liu, A. Luo, Z. Luo, and W. Xu, "High-repetition-rate pulsed fiber laser based on virtually imaged phased array," Chin. Opt. Lett. **18**, 071403 (2020).
12. A. Martinez and S. Yamashita, "Multi-gigahertz repetition rate passively modelocked fiber lasers using carbon nanotubes," Opt. Express **19**, 6155 (2011).
13. A. M. Smirnov, A. P. Bazakutsa, Y. K. Chamorovskiy, I. A. Nechepurenko, A. V. Dorofeenko, and O. V. Butov, "Thermal switching of lasing regimes in heavily doped Er^{3+} fiber lasers," ACS Photon. **5**, 5038 (2018).
14. S. H. Xu, Z. M. Yang, T. Liu, W. N. Zhang, Z. M. Feng, Q. Y. Zhang, and Z. H. Jiang, "An efficient compact 300 mW narrow-linewidth single frequency fiber laser at 1.5 μm," Opt. Express **18**, 1249 (2010).
15. N. Boetti, D. Pugliese, E. Ceci-Ginistrelli, J. Lousteau, D. Janner, and D. Milanese, "Highly doped phosphate glass fibers for compact lasers and amplifiers: a review," Appl. Sci. **7**, 1295 (2017).
16. X. Gao, Z. Zhao, Z. Cong, G. Gao, A. Zhang, H. Guo, G. Yao, and Z. Liu, "Stable 5-GHz fundamental repetition rate passively SESAM mode-locked Er-doped silica fiber lasers," Opt. Express **29**, 9021 (2021).
17. B. J. Ainslie, "A review of the fabrication and properties of erbium-doped fibers for optical amplifiers," J. Lightwave Technol. **9**, 220 (1991).
18. E. Maurice, G. Monnom, B. Dussardier, and D. B. Ostrowsky, "Clustering-induced nonsaturable absorption phenomenon in heavily erbium-doped silica fibers," Opt. Lett. **20**, 2487 (1995).
19. D. Boivin, T. Föhn, E. Burov, A. Pastouret, C. Gonnet, O. Cavani, C. Collet, and S. Lempereur, "Quenching investigation on new erbium doped fibers using MCVD nanoparticle doping process," Proc. SPIE **7580**, 75802B (2010).
20. P. G. Rojas Hernandez, M. Belal, C. Baker, S. Pidishety, Y. Feng, E. J. Friebele, L. B. Shaw, D. Rhonehouse, J. Sanghera, and J. Nilsson, "Efficient extraction of high pulse energy from partly quenched highly Er^{3+}-doped fiber amplifiers," Opt. Express **28**, 17124 (2020).
21. A. Dhar, A. Pal, M. C. Paula, P. Ray, H. S. Maiti, and R. Sen, "The mechanism of rare earth incorporation in solution doping process," Opt. Express **16**, 12835 (2008).
22. Y. Jiao, M. Guo, R. Wang, C. Shao, and L. Hu, "Influence of Al/Er ratio on the optical properties and structures of Er^{3+}/Al^{3+} co-doped silica glasses," J. Appl. Phys. **129**, 053104 (2021).
23. C. Yang, X. Guan, W. Lin, Q. Zhao, G. Tang, J. Gan, Q. Qian, Z. Feng, Z. Yang, and S. Xu, "Efficient 1.6 μm linearly-polarized single-frequency phosphate glass fiber laser," Opt. Express **25**, 29078 (2017).
24. K. Linganna, J.-H. In, J.-T. Ahn, Y. Choi, Y.-E. Im, D.-B. Kim, and J. H. Choi, "Implementation of fluorophoshate laser glass for short length active fiber at 1.5 μm," Opt. Laser Technol. **127**, 106189 (2020).
25. S. Fu, X. Zhu, J. Wang, J. Wu, M. Tong, J. Zong, M. Li, K. Wiersma, A. Chavez-Pirson, and N. Peyghambarian, "L-band wavelength-tunable Er^{3+}-doped tellurite fiber lasers," J. Lightwave Technol. **38**, 1435 (2020).
26. O. N. Egorova, S. L. Semjonov, V. V. Velmiskin, Y. P. Yatsenko, S. E. Sverchkov, B. I. Galagan, B. I. Denker, and E. M. Dianov, "Phosphate-core silica-clad Er/Yb-doped optical fiber and cladding pumped laser," Opt. Express **22**, 7632 (2014).
27. B. I. Denker, B. I. Galagan, V. A. Kamynin, A. A. Ponosova, K. E. Riumkin, S. L. Semjonov, S. E. Sverchkov, and V. B. Tsvetkov, "Gain characteristics of fibers with a heavily erbium-doped phosphate-based core and silica cladding," J. Opt. Soc. Am. B **36**, 2705 (2019).
28. A. M. Smirnov and O. V. Butov, "Pump and thermal impact on heavily erbium-doped fiber laser generation," Opt. Lett. **46**, 86 (2020).
29. A. V. Kir'yanov, Y. O. Barmenkov, G. E. Sandoval-Romero, and L. Escalante-Zarate, "Er^{3+} concentration effects in commercial erbium-doped silica fibers fabricated through the MCVD and DND technologies," IEEE J. Quantum Electron. **49**, 511 (2013).
30. D. S. Fan, Y. H. Luo, B. B. Yan, A. Stancalie, D. Ighigeanu, D. Negut, D. Sporea, J. Z. Zhang, J. X. Wen, J. J. Ma, P. F. Lu, and G. D. Peng, "Ionizing radiation effect upon Er/Yb co-doped fibre made by *in-situ* nano solution doping," J. Lightwave Technol. **38**, 6334 (2020).
31. F. Wang, Z. Lin, C. Shao, Q. Zhou, L. Zhang, M. Wang, D. Chen, G. Gao, S. Wang, C. Yu, and L. Hu, "Centimeter-scale Yb-free heavily Er-doped silica fiber laser," Opt. Lett. **43**, 2356 (2018).
32. W. Li, Q. Zhou, L. Zhang, S. Wang, M. Wang, C. Yu, S. Feng, D. Chen, and L. Hu, "Watt-level Yb-doped silica glass fiber laser with a core made by sol-gel method," Chin. Opt. Lett. **11**, 091601 (2013).
33. P. Myslinski, J. Fraser, and J. Chrostowski, "Nanosecond kinetics of upconversion process in EDF and its effect on EDFA performance," in *Optical Amplifiers and Their Applications* (1995), paper ThE3.